Proceedings of Computational Engineering Conference JSCES
Vol. 28, 2023 May

Subloading surface model with super-yield surface for soils

Koichi Hashiguchi
Dr. Eng., Solids & Structure Solutions, Ltd. (Emeritus Professor of Kyushu University)
(6-13-1002, Kuromon, Chuo-ku, Fukuoka, Japan, E-mail: hashikoi87@gmail.com)

The subloading surface model for soils with the super-yield surface, called the SYS model, is formulated in this article. The existing formulation of the SYS model is revised basically on various aspects, i.e. the finite plastic volumetric strain and the applicability to the negative pressure range, the cyclic loading, the rotational hardening, etc.

Key Words : *Cyclic loading, Elastoplasticity, Rotational hardening, Soil, Subloading surface, Super-yield surface*

1. INTRODUCTION

The description of the soil deformation behavior by the Cam-clay model [1][2] (even with Drucker-Prager model [3]) is improved drastically by the subloading surface model (Hashiguchi [4]-[6]) as shown by Hashiguchi and Chen [7], Hashiguchi et al. [8], etc. However, the deformation behaviors of sands in different void ratios cannot be described by a unique set of values of the material parameters and the undrained deformation behavior of sands cannot be described appropriately by the existing formulation of the subloading surface model. In this situation the idea of the incorporation of the *super-yield surface* into the subloading surface model, called the *SYS model*, was proposed by Asaoka et al. [9]-[12] in order to describe these behaviors by a unique set of material parameters. The main idea of the SYS model is that the loose sands and the naturally deposited clays possess the skeleton structures causing the large yielding strength. Unfortunately, however, the existing formulation of the SYS model is quite primitive involving various shortcomings as some of them are described in the following

1) It is based on the linear relation of the void-ratio vs. logarithmic of the pressure, although the linear relation of the both logarithmic of volume and pressure (Hashiguchi [13][14]) must be adopted for the description of the finite volumetric deformation,
2) The yield surface is limited to the positive pressure range so that the deformations of soils subjected to the null pressure (observed in soil ground surfaces) and the negative pressure (observed in cohesive soils) cannot be described as indicated and modified by Hashiguchi and Mase [15]),
3) The influence of third deviatoric stress invariant in the yielding behavior as formulated by Hashiguchi [16] is not taken into account, although it is inevitable for the prediction of deformation behavior of frictional materials.
4) The irrational formulation for the induced anisotropy caused by the rotation of the yield surface (Ohta and Sekiguchi [17], Hashiguchi [18]) has been incorporated by Asaoka et al. [19] following Hashiguchi and Chen [7] in which the rate-linear rotational hardening rule is adopted, although the nonlinear evolution rule (Hashiguchi [21]; Hashiguchi et al. [22]) must be adopted.
5) The inappropriate evolution rule of the normal-yield ratio by the logarithmic function (Hashiguchi and Chen [7]) is adopted, while it has been modified to the cotangent function which possesses the strong stress-controlling function to pull-back the stress to the yield surface in the numerical calculation and the analytical integrability by the plastic strain (cf. Hashiguchi [6][20]).
6) The cyclic loading behavior cannot be described and thus the liquefaction phenomenon induced in earthquakes cannot be described appropriately, since the initial subloading surface model (Hashiguchi [4]) is adopted but the extended subloading surface model (Hashiguchi [5][6]) is not adopted, while the translation of the similarity-center of the normal-yield and the subloading surfaces is incorporated in the extended subloading surface model.

Thus, the explicit formulation of the SYS model has not been developed substantially since the early stage of the proposal in 2000 as seen in Asaoka [12] similarly to the Cam-clay model which has not been developed by the proposers themselves conservatively.

The extended subloading surface model with the super-yield surface will be formulated, in which all the above-mentioned defects involved in the existing SYS model are excluded.

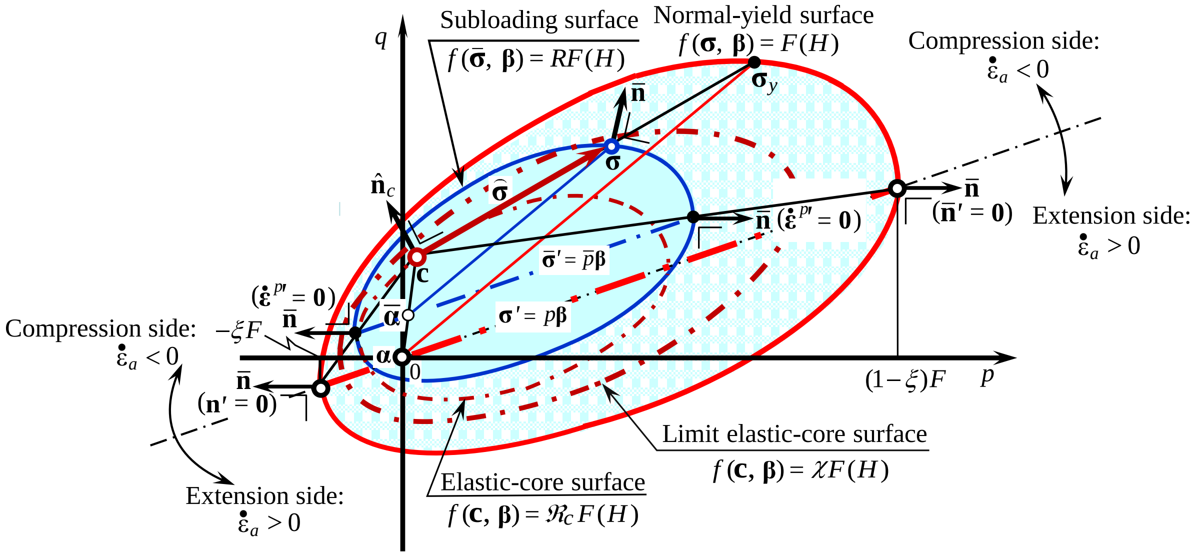

Fig. 1. Rotated normal-yield, subloading and similarity-center surfaces in the (p, q) plane.

2. SUPER-YIIELD, NORMAL-YIELD AND SUBLOADING SURFACES

The normal-yield and the subloading surfaces which is similar to the normal-yield and the super-yield surface and passes through the current stress for soils are given as follows (see **Fig. 1**):

$$f(\boldsymbol\sigma,\ \boldsymbol\beta) = F(H) \tag{1}$$

$$\boxed{f(\bar{\boldsymbol\sigma},\ \boldsymbol\beta) = RF(H)} \tag{2}$$

where the following relation holds by virtue of the similarity of the subloading surface to the normal-yield surface.

$$\bar{\boldsymbol\sigma} \equiv \boldsymbol\sigma - \bar{\boldsymbol\alpha}\ (= R\boldsymbol\sigma_y) = \hat{\boldsymbol\sigma} + R\mathbf{c} \tag{3}$$

with

$$\bar{\boldsymbol\alpha} \equiv (1-R)\mathbf{c}\quad (\bar{\boldsymbol\alpha} - \mathbf{c} = R(\boldsymbol\alpha - \mathbf{c});\ \boldsymbol\alpha = \mathbf{0}) \tag{4}$$

leading to

$$\dot{\bar{\boldsymbol\alpha}} = (1-R)\dot{\mathbf{c}} - \dot R\mathbf{c} \tag{5}$$

where

$$\hat{\boldsymbol\sigma} \equiv \boldsymbol\sigma - \mathbf{c} \tag{6}$$

$\boldsymbol\sigma$ is the Cauchy stress, $\boldsymbol\beta$ is the rotational hardening variable, $\mathbf{c}$ is the similarity-center of the subloading surface in Eq. (2) to the normal-yield (conventional yield) surface in Eq. (1), $\bar{\boldsymbol\alpha}$ in the subloading surface is the conjugate point to $\boldsymbol\alpha\ (=\mathbf{0})$ in the normal-yield surface as shown in the $(p,\ q)$ plane in **Fig. 1**, where $\boldsymbol\sigma_y$ on the normal-yield surface is the conjugate point to the current $\boldsymbol\sigma$ on the subloading surface. R is called the *normal-yield ratio*, designating the ratio of the size of the subloading surface to that of the size of the normal-yield surface. The rate of the rotational hardening is given as follows:

$$\dot{\boldsymbol\beta} = b_r\left(\dot{\boldsymbol\varepsilon}^{p\prime} - \frac{1}{\hat{\bar M}_r}\|\dot{\boldsymbol\varepsilon}^{p\prime}\|\boldsymbol\beta\right) = \mathbf{f}_{\beta\bar n}\dot\lambda \tag{7}$$

where

$$\hat{\bar M}_r(\cos3\theta_{\hat{\bar\sigma}}) = \frac{14\sqrt{6}\sin\phi_r}{(3-\sin\phi_r)(8+\cos3\theta_{\hat{\bar\sigma}})} \tag{8}$$

$$\hat{\bar{\boldsymbol\sigma}}' \equiv \bar{\boldsymbol\sigma}' - \bar p\boldsymbol\beta,\ \ \mathbf{t}'_{\hat{\bar\sigma}} \equiv \frac{\hat{\bar{\boldsymbol\sigma}}'}{\|\hat{\bar{\boldsymbol\sigma}}'\|},\ \ \cos3\theta_{\hat{\bar\sigma}} \equiv \sqrt{6}\,\mathrm{tr}\,\mathbf{t}'^{3}_{\hat{\bar\sigma}} \tag{9}$$

$$\mathbf{f}_{\beta\bar n} \equiv b_r\left(\bar{\mathbf{n}}' - \frac{1}{\hat{\bar M}_r}\|\bar{\mathbf{n}}'\|\boldsymbol\beta\right) \tag{10}$$

ϕ_r is the angle designating the limit of the rotation of the normal-yield surface.

Now, introduce the super-yield surface (Asaoka et al., [9]-[12]) (**Fig. 2**):

$$f(\boldsymbol\sigma,\ \boldsymbol\beta) = \bar R F(H) \tag{11}$$

where the plastic internal variable $\bar R\ (\geq 1)$ is the *super-normal-yield ratio* designating the ratio of the size of the *super-yield surface* to the size of the normal-yield surface, which represents the degree of the soil skeleton structure (larger in looser soils). The subloading surface is described as follows:

$$\boxed{f(\bar{\boldsymbol\sigma},\ \boldsymbol\beta) = \underline{R}\bar R F(H),\ \ R = \underline{R}\bar R} \tag{12}$$

where $\underline{R}\ (0 \leq \underline{R} \leq 1)$ is the *super-yield ratio* designating the ratio of the size of the subloading surface to the size of the super-yield surface. Here, note that the current stress can go over the normal-yield surface for structured soils.

Let the evolution rules of the super-normal yield ratio $\bar R$ based on the assumption that the super-yield surface shrinks by the deviatoric plastic strain rate and shrinks/expands by the plastic volumetric contraction/expansion and the super-yield ratio $\underline{R}$ based on the assumption that the subloading surface approaches the super-yield surface in the plastic loading process be given by

$$\dot{\bar R} = \bar U(\bar R)(\|\dot{\boldsymbol\varepsilon}^{p\prime}\| - c_v\dot\varepsilon_v^p),\ \ \dot{\underline{R}} = \underline{U}(\underline{R})\|\dot{\boldsymbol\varepsilon}^p\| \tag{13}$$

where

$$\bar{U}(\bar{R}) = -\bar{u}(\bar{R}^a - 1)\ (\le 0),\quad U(\underline{R}) = \underline{u}\cot\left(\frac{\pi}{2}\underline{R}\right)\ (\ge 0) \tag{14}$$

c_v (≤ 1), $\bar{u}$, a and $\underline{u}$ are the material constants and $\underline{u}$ is the material function which will be formulated later in Eq. (29). The material constant c_v would be larger in clays than sands.

The following relation holds for the rate of the normal yield ratio R in terms of the super-normal-yield ratio $\bar{R}$ and the super-yield ratio $\underline{R}$ hold from Eq. (13) with Eq. (14), noting Eq. (12).

$$\frac{\dot{R}}{R} = \frac{\dot{\bar{R}}}{\bar{R}} + \frac{\dot{\underline{R}}}{\underline{R}} = \frac{\bar{U}(\bar{R})}{\bar{R}}\left(\|\dot{\boldsymbol{\varepsilon}}^{p\prime}\| - c_v\dot{\varepsilon}_v^p\right) + \frac{U(\underline{R})}{\underline{R}}\|\dot{\boldsymbol{\varepsilon}}^p\|$$

$$= -\frac{\bar{u}(\bar{R}^a - 1)}{\bar{R}}\left(\|\dot{\boldsymbol{\varepsilon}}^{p\prime}\| - c_v\dot{\varepsilon}_v^p\right) + \frac{\underline{u}}{\underline{R}}\cot\left(\frac{\pi}{2}\underline{R}\right)\|\dot{\boldsymbol{\varepsilon}}^p\| \tag{15}$$

The undrained stress paths in loose and dense sands can be predicted by the SYS model with one same values of material parameters as shown in **Fig. 3** without resorting to the plastic deviatoric hardening (Nova [23]; Wilde [24]) as will be known from the plastic modulus shown in Eq. (36).

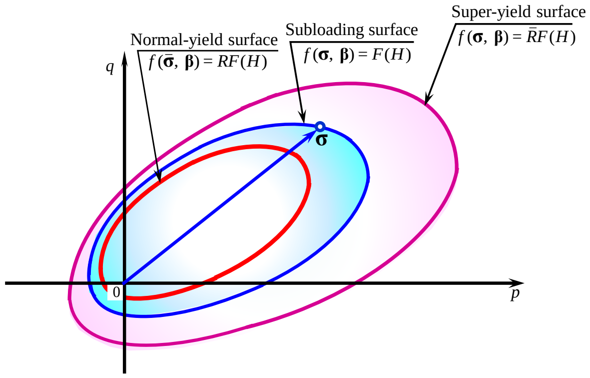

Fig. 2. Super-yield, normal-yield and subloading surfaces in the (p, q) plane.

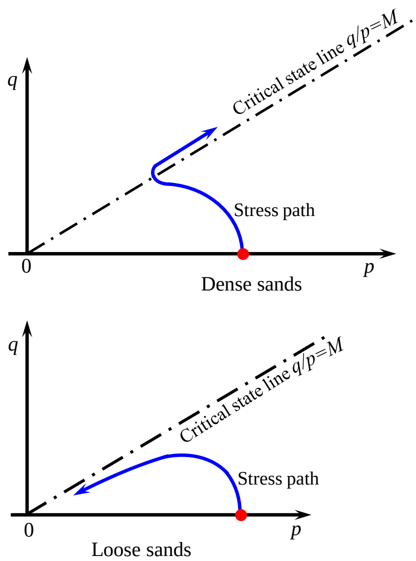

Fig. 3 Stress path under constant volume or undrained condition.

The material-time derivative of Eq. (2) reads:

$$\frac{\partial f(\bar{\boldsymbol{\sigma}}, \boldsymbol{\beta})}{\partial \bar{\boldsymbol{\sigma}}}:\dot{\boldsymbol{\sigma}} - \frac{\partial f(\bar{\boldsymbol{\sigma}}, \boldsymbol{\beta})}{\partial \bar{\boldsymbol{\sigma}}}:\dot{\boldsymbol{\alpha}} + \frac{\partial f(\bar{\boldsymbol{\sigma}}, \boldsymbol{\beta})}{\partial \boldsymbol{\beta}}:\dot{\boldsymbol{\beta}} = \dot{R}F + R\dot{F} \tag{16}$$

which can be rewritten as

$$\bar{\mathbf{n}}:\dot{\boldsymbol{\sigma}} - \bar{\mathbf{n}}:\left[\dot{\boldsymbol{\alpha}} + \frac{\dot{F}}{F}\bar{\boldsymbol{\sigma}} + \frac{\dot{R}}{R}\bar{\boldsymbol{\sigma}} - \frac{1}{RF}\left(\frac{\partial f(\bar{\boldsymbol{\sigma}}, \boldsymbol{\beta})}{\partial \boldsymbol{\beta}}:\dot{\boldsymbol{\beta}}\right)\bar{\boldsymbol{\sigma}}\right] = 0 \tag{17}$$

where

$$\bar{\mathbf{n}} \equiv \frac{\partial f(\bar{\boldsymbol{\sigma}}, \boldsymbol{\beta})}{\partial \bar{\boldsymbol{\sigma}}} \Big/ \left\|\frac{\partial f(\bar{\boldsymbol{\sigma}}, \boldsymbol{\beta})}{\partial \bar{\boldsymbol{\sigma}}}\right\| \quad (\|\bar{\mathbf{n}}\| = 1) \tag{18}$$

noting the following equation based on the Euler's theorem for the function of $\bar{\boldsymbol{\sigma}}$ in homogeneous degree-one.

$$\frac{1}{\dfrac{\partial f(\bar{\boldsymbol{\sigma}}, \boldsymbol{\beta})}{\partial \bar{\boldsymbol{\sigma}}}} = \frac{\dfrac{\partial f(\bar{\boldsymbol{\sigma}}, \boldsymbol{\beta})}{\partial \bar{\boldsymbol{\sigma}}}:\bar{\boldsymbol{\sigma}}}{\bar{\mathbf{n}}:\bar{\boldsymbol{\sigma}}}\bar{\mathbf{n}} = \frac{f(\bar{\boldsymbol{\sigma}}, \boldsymbol{\beta})}{\bar{\mathbf{n}}:\bar{\boldsymbol{\sigma}}}\bar{\mathbf{n}} = \frac{RF}{\bar{\mathbf{n}}:\bar{\boldsymbol{\sigma}}}\bar{\mathbf{n}} \tag{19}$$

3. EVOLUTION RULE OF ELASTIC-CORE

To avoid the unlimited approach of the elastic-core to the normal-yield surface, first let the following surface, called the *elastic-core surface*, be introduced as shown in Fig. 1, which passes through the elastic-core $\mathbf{c}$ and possesses a similar shape and orientation to the normal-yield surface with respect to the null stress $(\boldsymbol{\sigma} = \boldsymbol{\alpha} = \mathbf{0})$.

$$f(\mathbf{c}, \boldsymbol{\beta}) = \mathfrak{R}_c F(H),\quad \mathfrak{R}_c = f(\mathbf{c}, \boldsymbol{\beta})/F(H) \tag{20}$$

where the variable $\mathfrak{R}_c$ is the ratio of the size of the elastic-core surface to that of the normal-yield surface, called the *elastic-core yield ratio*. It plays the role of a measure for the approaching degree of the elastic-core to the normal-yield surface. Since the elastic-core must lie inside the normal-yield surface as described above, the elastic-core yield ratio has to be less than unity. Then, the inequality

$$f(\mathbf{c}, \boldsymbol{\beta}) \le \chi F(H),\ \text{i.e. } \mathfrak{R}_c \le \chi \tag{21}$$

must hold, where χ (<1) is a material constant exhibiting the maximum value of $\mathfrak{R}_c$. The time-differentiation of Eq. (21) at the limit state in which $\mathbf{c}$ lies on the *limit elastic-core surface* $f(\mathbf{c}, \boldsymbol{\beta}) = \chi F(H)$ yields

$$\frac{\partial f(\mathbf{c}, \boldsymbol{\beta})}{\partial \mathbf{c}}:\dot{\mathbf{c}} + \frac{\partial f(\mathbf{c}, \boldsymbol{\beta})}{\partial \boldsymbol{\beta}}:\dot{\boldsymbol{\beta}} - \chi\dot{F} \le 0 \quad \text{for } \mathfrak{R}_c = \chi$$

which can be rewritten as

$$\frac{\partial f(\mathbf{c}, \boldsymbol{\beta})}{\partial \mathbf{c}}:\dot{\mathbf{c}} + \left(\frac{1}{\chi F}\frac{\partial f(\mathbf{c}, \boldsymbol{\beta})}{\partial \mathbf{c}}:\mathbf{c}\right)\frac{\partial f(\mathbf{c}, \boldsymbol{\beta})}{\partial \boldsymbol{\beta}}:\dot{\boldsymbol{\beta}}$$

$$-\left(\frac{1}{\chi F}\frac{\partial f(\mathbf{c}, \boldsymbol{\beta})}{\partial \mathbf{c}}:\mathbf{c}\right)\chi\dot{F} \le 0 \quad \text{for } \mathfrak{R}_c = \chi \tag{22}$$

Making use of the relation $[\partial f(\mathbf{c}, \boldsymbol{\beta})/\partial \mathbf{c}]:\mathbf{c}$ $(= f(\mathbf{c}, \boldsymbol{\beta})) = \chi F$ on account of the Euler's homogeneous function $f(\mathbf{c}, \boldsymbol{\beta})$ of $\mathbf{c}$ in degree-one, Eq. (22) is further rewritten as

$$\frac{\partial f(\mathbf{c},\boldsymbol{\beta})}{\partial \mathbf{c}}:\Big[\overset{\bullet}{\mathbf{c}}+\Big(\frac{1}{\chi F}\frac{\partial f(\mathbf{c},\boldsymbol{\beta})}{\partial \boldsymbol{\beta}}:\overset{\bullet}{\boldsymbol{\beta}}-\frac{\overset{\bullet}{F}}{F}\Big)\mathbf{c}\Big]\le 0 \quad \text{for } \mathscr{R}_c=\chi \tag{23}$$

Equations (21) and (23) (rate form) are called the *enclosing condition of elastic-core*. Let the following relation be adopted.

$$\overset{\bullet}{\mathbf{c}}+\Big(\frac{1}{\chi F}\frac{\partial f(\mathbf{c},\boldsymbol{\beta})}{\partial \boldsymbol{\beta}}:\overset{\bullet}{\boldsymbol{\beta}}-\frac{\overset{\bullet}{F}}{F}\Big)\mathbf{c}=c_e\|\overset{\bullet}{\boldsymbol{\varepsilon}}{}^p\|(\boldsymbol{\sigma}_\chi-\mathbf{c}) \tag{24}$$

where c_e is the material constant controlling the translational rate of the elastic-core and $\boldsymbol{\sigma}_\chi$ on the limit elastic-core surface is the conjugate point to the current stress $\boldsymbol{\sigma}$ on the subloading surface, i.e.

$$\boldsymbol{\sigma}_\chi=\frac{\chi}{R}\bar{\boldsymbol{\sigma}}\quad\left(\frac{\bar{\boldsymbol{\sigma}}}{R}\Big(=\frac{\boldsymbol{\sigma}-\bar{\boldsymbol{\alpha}}}{R}\Big)=\frac{\boldsymbol{\sigma}_\chi-\boldsymbol{\alpha}}{\chi}=\frac{\boldsymbol{\sigma}_\chi}{\chi}\right) \tag{25}$$

The inequality in Eq. (23) is fulfilled in Eq. (24) as verified by

$$\frac{\partial f(\mathbf{c},\boldsymbol{\beta})}{\partial \mathbf{c}}:[c_e\|\overset{\bullet}{\boldsymbol{\varepsilon}}{}^p\|(\boldsymbol{\sigma}_\chi-\mathbf{c})]$$
$$=c_e\|\overset{\bullet}{\boldsymbol{\varepsilon}}{}^p\|\frac{\partial f(\mathbf{c},\boldsymbol{\beta})}{\partial \mathbf{c}}:(\boldsymbol{\sigma}_\chi-\mathbf{c})\le 0 \quad \text{for } \mathscr{R}_c=\chi \tag{26}$$

noting that $\partial f(\mathbf{c},\boldsymbol{\beta})/\partial\mathbf{c}$ is the outward-normal of the elastic-core surface at the current elastic-core $\mathbf{c}$ and makes an obtuse angle with $\boldsymbol{\sigma}_\chi-\mathbf{c}$ when $\mathbf{c}$ lies on the limit elastic-core surface $f(\mathbf{c},\boldsymbol{\beta})=\chi F(H)$ as far as it is the convex surface, while $\boldsymbol{\sigma}_\chi$ lies on the limit elastic-core surface.

Consequently, the following evolution rule of $\mathbf{c}$ is given from Eq. (24) with Eq. (25) as follows:

$$\overset{\bullet}{\mathbf{c}}=c_e\|\overset{\bullet}{\boldsymbol{\varepsilon}}{}^p\|\Big(\frac{\chi}{R}\bar{\boldsymbol{\sigma}}-\mathbf{c}\Big)+\Big(\frac{\overset{\bullet}{F}}{F}-\frac{1}{\chi F}\frac{\partial f(\mathbf{c},\boldsymbol{\beta})}{\partial \boldsymbol{\beta}}:\overset{\bullet}{\boldsymbol{\beta}}\Big)\mathbf{c} \tag{27}$$

The substitution of Eq. (27) into Eq. (5) leads to

$$\overset{\bullet}{\bar{\boldsymbol{\alpha}}}=(1-R)\Big[c_e\|\overset{\bullet}{\boldsymbol{\varepsilon}}{}^p\|\Big(\frac{\chi}{R}\bar{\boldsymbol{\sigma}}-\mathbf{c}\Big)+\Big(\frac{\overset{\bullet}{F}}{F}-\frac{1}{\chi F}\frac{\partial f(\mathbf{c},\boldsymbol{\beta})}{\partial \boldsymbol{\beta}}:\overset{\bullet}{\boldsymbol{\beta}}\Big)\mathbf{c}\Big]-\overset{\bullet}{R}\mathbf{c} \tag{28}$$

In order to improve the reloading behavior such that the reloading curve recover to the preceding loading curve promptly, the material function $\underline{u}$ in Eq. $(14)_2$ is given by

$$\underline{u}=u\exp(u_c\mathscr{R}_c C_n) \tag{29}$$

where u is the material constant and

$$C_n\equiv\mathbf{n}_c:\bar{\mathbf{n}}\quad(-1\le C_n\le 1) \tag{30}$$

$$\mathbf{n}_c\equiv\frac{\partial f(\mathbf{c},\boldsymbol{\beta})}{\partial \mathbf{c}}\Big/\Big\|\frac{\partial f(\mathbf{c},\boldsymbol{\beta})}{\partial \mathbf{c}}\Big\|\quad(\|\mathbf{n}_c\|=1) \tag{31}$$

4. PLASTIC STRAIN RATE

The substitution of Eq. (28) into Eq. (17) leads to the consistency condition:

$$\bar{\mathbf{n}}:\overset{\bullet}{\boldsymbol{\sigma}}-\bar{\mathbf{n}}:\Big\{(1-R)\Big[c_e\|\overset{\bullet}{\boldsymbol{\varepsilon}}{}^p\|\Big(\frac{\chi}{R}\bar{\boldsymbol{\sigma}}-\mathbf{c}\Big)+\Big(\frac{\overset{\bullet}{F}}{F}-\frac{1}{\chi F}\frac{\partial f(\mathbf{c},\boldsymbol{\beta})}{\partial \boldsymbol{\beta}}:\overset{\bullet}{\boldsymbol{\beta}}\Big)\mathbf{c}\Big]-\overset{\bullet}{R}\mathbf{c}+\frac{\overset{\bullet}{F}}{F}\bar{\boldsymbol{\sigma}}+\frac{\overset{\bullet}{R}}{R}\bar{\boldsymbol{\sigma}}-\frac{1}{RF}\Big(\frac{\partial f(\bar{\boldsymbol{\sigma}},\boldsymbol{\beta})}{\partial \boldsymbol{\beta}}:\overset{\bullet}{\boldsymbol{\beta}}\Big)\bar{\boldsymbol{\sigma}}\Big\}=0$$

i.e.

$$\bar{\mathbf{n}}:\overset{\bullet}{\boldsymbol{\sigma}}-\bar{\mathbf{n}}:\Big[c_e(1-R)\|\overset{\bullet}{\boldsymbol{\varepsilon}}{}^p\|\Big(\frac{\chi}{R}\bar{\boldsymbol{\sigma}}-\mathbf{c}\Big)+\frac{\overset{\bullet}{F}}{F}[\bar{\boldsymbol{\sigma}}+(1-R)\mathbf{c}]+\frac{\overset{\bullet}{R}}{R}(\bar{\boldsymbol{\sigma}}-R\mathbf{c})-\frac{1}{RF}\Big(\frac{\partial f(\bar{\boldsymbol{\sigma}},\boldsymbol{\beta})}{\partial \boldsymbol{\beta}}:\overset{\bullet}{\boldsymbol{\beta}}\Big)\bar{\boldsymbol{\sigma}}-\frac{1-R}{\chi F}\Big(\frac{\partial f(\mathbf{c},\boldsymbol{\beta})}{\partial \boldsymbol{\beta}}:\overset{\bullet}{\boldsymbol{\beta}}\Big)\mathbf{c}\Big]=0 \tag{32}$$

By virtue of the relations

$$\begin{cases}\bar{\boldsymbol{\sigma}}+(1-R)\mathbf{c}=\boldsymbol{\sigma}\\ \bar{\boldsymbol{\sigma}}-R\mathbf{c}=\hat{\boldsymbol{\sigma}}\end{cases}$$

deduced from Eq. (3), Eq. (32) is simplified to the equation:

$$\bar{\mathbf{n}}:\overset{\bullet}{\boldsymbol{\sigma}}-\bar{\mathbf{n}}:\Big[c_e(1-R)\|\overset{\bullet}{\boldsymbol{\varepsilon}}{}^p\|\Big(\frac{\chi}{R}\bar{\boldsymbol{\sigma}}-\mathbf{c}\Big)+\frac{\overset{\bullet}{F}}{F}\boldsymbol{\sigma}+\frac{\overset{\bullet}{R}}{R}\hat{\boldsymbol{\sigma}}-\frac{1}{RF}\Big(\frac{\partial f(\bar{\boldsymbol{\sigma}},\boldsymbol{\beta})}{\partial \boldsymbol{\beta}}:\overset{\bullet}{\boldsymbol{\beta}}\Big)\bar{\boldsymbol{\sigma}}-\frac{1-R}{\chi F}\Big(\frac{\partial f(\mathbf{c},\boldsymbol{\beta})}{\partial \boldsymbol{\beta}}:\overset{\bullet}{\boldsymbol{\beta}}\Big)\mathbf{c}\Big]=0 \tag{33}$$

Substituting the plastic strain rate $\overset{\bullet}{\boldsymbol{\varepsilon}}{}^p$ in the associated flow rule

$$\overset{\bullet}{\boldsymbol{\varepsilon}}{}^p=\overset{\bullet}{\bar{\lambda}}\bar{\mathbf{n}} \tag{34}$$

where $\overset{\bullet}{\bar{\lambda}}$ is the positive proportionality factor into Eq. (33) with Eq. (15), one has

$$\overset{\bullet}{\bar{\lambda}}=\frac{\bar{\mathbf{n}}:\overset{\bullet}{\boldsymbol{\sigma}}}{\bar{M}^p}\bar{\mathbf{n}} \tag{35}$$

where

$$\bar{M}^p\equiv\bar{\mathbf{n}}:\Big[\frac{F' f_{H\bar{n}}}{F}\boldsymbol{\sigma}+\Big(\frac{\bar{U}(\bar{R})}{\bar{R}}(\|\bar{\mathbf{n}}'\|-c_v\mathrm{tr}\bar{\mathbf{n}})+\frac{\underline{U}(\underline{R})}{\underline{R}}\Big)\hat{\boldsymbol{\sigma}}+c(1-R)\Big(\frac{\chi}{R}\bar{\boldsymbol{\sigma}}-\mathbf{c}\Big)-\frac{1}{RF}\Big(\frac{\partial f(\bar{\boldsymbol{\sigma}},\boldsymbol{\beta})}{\partial \boldsymbol{\beta}}:\mathbf{f}_{\beta\bar{n}}\Big)\bar{\boldsymbol{\sigma}}-\frac{1-R}{\chi F}\Big(\frac{\partial f(\mathbf{c},\boldsymbol{\beta})}{\partial \boldsymbol{\beta}}:\mathbf{f}_{\beta\bar{n}}\Big)\mathbf{c}\Big] \tag{36}$$

Therefore, the softening is induced in the loose soils in the over-normally-consolidated state for which the structure of soil skeleton is highly developed leading to $\bar{R}\gg 1,\ \bar{U}(\bar{R})\ll 0$ and $\underline{R}\cong 1,\ \underline{U}(\underline{R})\cong 0\rightarrow\bar{M}^p<0$ as shown in Fig. 3. On the other hand, the hardening is induced in the dense soil under the over-consolidated sate for which the structure of soil skeleton is not developed leading to $\bar{R}\cong 1,\ \bar{U}(\bar{R})\cong 0$ and $\underline{R}\ll 1,\ \underline{U}(\underline{R})\gg 0\rightarrow\bar{M}^p>0$ as shown in Fig. 3. Consider the cyclic loading of the infinitesimal stress amplitude under the drained condition at the isotropic stress state in the loose soil. The structure of soil skeleton tends to decrease because of $\overset{\bullet}{\bar{R}}<0$ and the over-consolidation tends to increase leading to the dense soil because of $\overset{\bullet}{\varepsilon}{}_v^p<0\rightarrow\overset{\bullet}{F}>0$. The details can be referred to Hashiguchi [25]).

The plastic strain rate, the strain rate and the stress rate are given by Eqs. (34) and (35).

$$\overset{\circ}{\boldsymbol{\varepsilon}} = \mathbb{E}^{-1} : \overset{\circ}{\boldsymbol{\sigma}} + \dot{\lambda}\bar{\mathbf{n}} = \left(\mathbb{E}^{-1} + \frac{\bar{\mathbf{n}} \otimes \bar{\mathbf{n}}}{\bar{M}^{p}}\right) : \overset{\circ}{\boldsymbol{\sigma}} \tag{37}$$

$$\overset{\circ}{\boldsymbol{\sigma}} = \mathbb{E} : \overset{\circ}{\boldsymbol{\varepsilon}} - \dot{\Lambda}\mathbb{E} : \bar{\mathbf{n}} = \left(\mathbb{E} - \frac{\mathbb{E} : \bar{\mathbf{n}} \otimes \bar{\mathbf{n}} : \mathbb{E}}{\bar{M}^{p} + \bar{\mathbf{n}} : \mathbb{E} : \bar{\mathbf{n}}}\right) : \overset{\circ}{\boldsymbol{\varepsilon}} \tag{38}$$

where

$$\dot{\Lambda} = \frac{\bar{\mathbf{n}} : \mathbb{E} : \overset{\circ}{\boldsymbol{\varepsilon}}}{\bar{M}^{p} + \bar{\mathbf{n}} : \mathbb{E} : \bar{\mathbf{n}}}, \quad \overset{\circ}{\boldsymbol{\varepsilon}}^{p} = \frac{\bar{\mathbf{n}} : \mathbb{E} : \overset{\circ}{\boldsymbol{\varepsilon}}}{\bar{M}^{p} + \bar{\mathbf{n}} : \mathbb{E} : \bar{\mathbf{n}}}\bar{\mathbf{n}} \tag{39}$$

$\mathbb{E}$ is the elastic modulus tensor.

The loading criterion is given by

$$\begin{cases} \overset{\circ}{\boldsymbol{\varepsilon}}^{p} \neq \mathbf{O} \text{ for } \dot{\Lambda} > 0 \text{ or } \bar{\mathbf{n}} : \mathbb{E} : \overset{\circ}{\boldsymbol{\varepsilon}} > 0 \\ \overset{\circ}{\boldsymbol{\varepsilon}}^{p} = \mathbf{O} \text{ for others} \end{cases} \tag{40}$$

う

ACKNOWLEDGMENT: The author expresses the deep gratitude to Prof. Toshihiro NODA and Dr. Kentaro NAKAI, Nagoya Univ. for providing the valuable research papers on the SYS model and their doctoral theses to him.

REFERENCES

[1] Roscoe, K. H. and Burland, J. B. (1968): On the generalized stress-strain behaviour of 'wet' clay, *Engineering Plasticity*, Cambridge Univ. Press, Cambridge, pp. 535-608.

[2] Schofield, A. N. and Wroth, C. P. (1968): *Critical State Soil Mechanics*, McGraw-Hill, London.

[3] Drucker, D. C. and Prager, W. (1952): Soil mechanics and plastic analysis or limit design, *Quart. Appl. Math*., **10**, 157-165.

[4] Hashiguchi, K. (1980): Constitutive equations of elastoplastic materials with elastic-plastic transition, *J. Appl. Mech*. (ASME), **47**, 266-272.

[5] Hashiguchi, K. (1989): Subloading surface model in unconventional plasticity, *Int. J. Solids Structures*, **25**, 917-945.

[6] Hashiguchi, K. (2023): *Foundations of Elastoplasticity: Subloading Surface Model*, Springer.

[7] Hashiguchi, K. and Chen, Z.-P (1998): Elastoplastic constitutive equations of soils with the subloading surface and the rotational hardening, *Int. J. Numer. Anal. Meth. Geomech*., **22**, 197-227.

[8] Hashiguchi, K., Saitoh, K., Okayasu, T. and Tsutsumi, S. (2002): Evaluation of typical conventional and unconventional plasticity models for prediction of softening behavior of soils, *Geotechnique*, **52**, 561-573.

[9] Asaoka, A., Nakano, M. and Noda, T. (1997): Soil-water coupled behaviour of heavily-overconsolidated clay near/at critical state, *Soils & Found.*, **37**(1), 13-28.

[10] Asaoka, A., Nakano, M. and Noda, T. (2000): Superloading yield surface concept for highly structured soil behavior, *Soils & Found.*, **40**(2), 99-110.

[11] Asaoka, A., Noda, T., Yamada, E., Kaneda, I and Nakano, M. (2002): An elasto-plastic description of two distinct volume change mechanics of soils, *Soils & Found.*, **42**(5), 99-110.

[12] Asaoka, A. (2023): My road in research of elastoplastic soil mechanics, *Soils & Found.*, **63**, 101294.

[13] Hashiguchi, K. (1974): Isotropic hardening theory of granular media, *Proc. Japan. Soc. Civil Eng.*, No. 227, 45-60. (in Japanese)

[14] Hashiguchi, K. and Ueno, M. (1977): Elastoplastic constitutive laws of granular materials, *Constitutive Equations of Soils* (*Proc. 9th Int. Conf. Soil Mech. Found. Eng., Spec. Ses. 9*, S. Murayama and A.N. Schofield (eds.), Tokyo, JSSMFE, pp. 73-82.

[15] Hashiguchi, K. and Mase, T. (2007): Extended yield condition of soils with tensile strength and rotational hardening, *Int. J. Plasticity*, **23**, 1939-1956.

[16] Hashiguchi, K. (2002): A proposal of the simplest convex-conical surface for soils, *Soils and Foundations*, **42**(3), 107-113.

[17] Sekiguchi, H. and Ohta, H. (1977): Induced anisotropy and its time dependence in clays, *Constitutive Equations of Soils (Proc. Spec. Session 9, 9th ICSFME)*, Tokyo, pp. 229-238.

[18] Hashiguchi, K. (1977): An expression of anisotropy in a plastic constitutive equation of soils, *Constitutive Equations of Soils* (*Proc. 9th Int. Conf. Soil Mech. Found. Eng., Spec. Ses. 9*, (eds. Murayama, S. and Schofield, A.N.), Tokyo, JSSMFE, pp. 302-305.

[19] Asaoka, A., Noda, T. Yamada, E., Kaneda, K. and Nakano, M., *Soils and Foundations*, **42**, 47-57.

[20] Hashiguchi, K. (2014): *Elastoplasticity Theory*, Second edition, Springer.

[21] Hashiguchi, K. (2017): *Foundations of Elastoplasticity: Subloading Surface Model*, First Edition, Springer.

[22] Hashiguchi, K., Mase, T. and Yamakawa, Y. (2021): Elaborated subloading surface model for accurate description of cyclic mobility in granular materials, *Acta Geotech.*, https://doi.org/10.1007/s11440-021-021203-y

[23] Nova, R. (1977): On the hardening of soils, *Arch. Mech. Stos*., **29**, 445-458.

[24] Wilde, P. (1977): Two invariants depending models of granular media, *Arch. Mech. Stos*., **29**, 799-809.

[25] Hashiguchi, K. (2009): *Elastoplasticity Theory*, Springer.